AJNR

Visualization of intracranial aneurysms treated with Woven EndoBridge (WEB) devices using Ultrashort Echo Time Magnetic Resonance Imaging (UTE-MRI)

Daniel Toth, Stefan Sommer, Riccardo Ludovichetti, Markus Klarhöfer, Jawid Madjidyar, Patrick Thurner, Marco Piccirelli, Miklos Krepuska, Tim Finkenstädt, Roman Guggenberger, Sebastian Winklhofer, Zsolt Kulcsar and Tilman Schubert

AJNR Am J Neuroradiol published online 12 July 2024
http://www.ajnr.org/content/early/2024/07/03/ajnr.A8401

Published July 12, 2024 as 10.3174/ajnr.A8401

ORIGINAL RESEARCH

Visualization of intracranial aneurysms treated with Woven EndoBridge (WEB) devices using Ultrashort Echo Time Magnetic Resonance Imaging (UTE-MRI)

Daniel Toth, Stefan Sommer, Riccardo Ludovichetti, Markus Klarhöfer, Jawid Madjidyar, Patrick Thurner, Marco Piccirelli , Miklos Krepuska, Tim Finkenstädt, Roman Guggenberger, Sebastian Winklhofer, Zsolt Kulcsar, Tilman Schubert

ABSTRACT

BACKGROUND AND PURPOSE: Assessing treatment success of intracranial aneurysms treated with Woven EndoBridge (WEB) devices using MRI is important in follow-up imaging. Depicting both the device configuration as well as reperfusion is challenging due to susceptibility artefacts. We evaluated the usefulness of contrast-enhanced 3D-Ultrashort Echo-Time (UTE) sequence in this setting.

MATERIALS AND METHODS: In this prospective study, 12 patients (9 female) with 15 treated aneurysms were included. These 12 patients underwent 18 MRI examinations. Follow-up UTE-MRI controls were performed on the same 3-Tesla scanner. We compared the visualization of device configuration, artifact-related virtual stenosis of the parent vessel and WEB occlusion scale in 3D isotropic UTE-MRI post-contrast with standard time-of-flight (TOF) MR-angiography with (CE) and without intravenous contrast as well as DSA. Two interventional neuroradiologists rated the images separately and in consensus.

RESULTS: Visualization of the WEB device position and configuration was rated superior or highly superior using the UTE sequence in 17/18 MRIs compared to TOF-MRA. Artifact-related virtual stenosis of the parent vessel was significantly lower in UTE-MRI compared to TOF and CE-TOF. Reperfusion was visible in 8/18 controls in DSA. TOF was able to grade reperfusion correctly in 16 cases, CE-TOF in 16 cases and UTE in 17 cases.

CONCLUSIONS: Contrast-enhanced UTE is a novel MRI sequence that shows benefit compared to standard sequences in non-invasive and radiation-free follow-up imaging of intracranial aneurysms treated using the WEB-device.

ABBREVIATIONS: ACoA = anterior communicating artery, BA = basilar artery, CEA = contrast enhanced angiography, ICA = internal carotid artery, MCA = middle cerebral artery, PCom = posterior communicating artery TOF-CE = contrast enhanced time-of-flight angiography, UTE = ultra-short echo time, WEB = woven endobridge

Received month day, year; accepted after revision month day, year.

From the Department of Neuroradiology, Clinical Neuroscience Center, University Hospital Zürich, Zürich, Switzerland (D.T., J.W., R.L., P.T., M.P., M.K., S.W., Z.K., T.S.), Siemens Healthcare, Zürich, Switzerland (S.S., M.K.), and Advanced Clinical Imaging Technology (ACIT), Siemens Healthcare, Lausanne, Switzerland (S.S.), Department of Radiology, University Hospital Zürich, Zürich, Switzerland (R.G., T.F.)

S.S. and M.K. are employees of Siemens Healthcare.

.

Please address correspondence to Tilman Schubert, MD, Department of Neuroradiology, Clinical Neuroscience Center, University Hospital Zürich, Frauenklinikstrasse 10, 8091 Zürich, Switzerland, e-mail: tilman.schubert@usz.ch.

SUMMARY SECTION

PREVIOUS LITERATURE: Previous studies have explored the limitations of conventional MRI sequences in visualizing intracranial aneurysms treated with endovascular devices due to susceptibility artifacts. Time-of-Flight (TOF) MRI, including contrast-enhanced TOF (CE-TOF), often suffers from artifacts that obscure critical details of the device and adjacent vessels. Studies have shown the potential of ultrashort echo-time (UTE) MRI to mitigate these issues, offering better visualization of metal implants used in various aneurysm treatments, such as stents and coils, through reduced susceptibility artifacts.

KEY FINDINGS: UTE-MRI provides superior visualization of WEB devices and adjacent vessels compared to TOF-MRA, with significantly less artifact-related virtual stenosis and accurate assessment of aneurysm occlusion.

KNOWLEDGE ADVANCEMENT: This study demonstrates that UTE-MRI enhances follow-up imaging for intracranial aneurysms treated with WEB devices, improving the ability to assess device configuration and vessel patency, potentially guiding better clinical management.

Copyright 2024 by American Society of Neuroradiology.

INTRODUCTION

The treatment of wide necked aneurysms, which constitute up to 54% of intracranial aneurysms [12] may be challenging due to the proximity of branching vessels [3]. Besides surgical clipping, several endovascular methods have been employed, including coiling with temporary or permanent stent assistance or deployment of a flow diverting stent. One of the more recent options is the Woven EndoBridge device (WEB; Microvention/Terumo, Aliso Viejo, California), an intrasaccular flow disrupting device, which has been introduced for clinical use in 2011 [4]. WEB-devices have been successfully used in a number of locations, including the anterior communicating artery (ACoA), the middle cerebral artery (MCA), the internal carotid artery (ICA) and the basilar artery (BA).

Equivalent to other intracranial aneurysm treatment options, interval follow-up imaging for monitoring of aneurysm residual filling recurrence and complications such as occlusion of branching vessels is mandatory. The gained information is necessary for planning further follow-up intervals, adjusting anticoagulant medication regimens and determining the need for re-treatment [5, 6]. Due to the compact micro-wire braiding, which makes up the WEB-device, the information gained with computed tomography and magnetic resonance imaging (MRI) will be by limited beam hardening and susceptibility artefacts, respectively [7, 8]. Ideally, MRA would be able to show the configuration of the WEB device, which may experience infolding at the base, aneurysm recanalization along the aneurysm walls and, rarely, dislocation. Furthermore, branch vessels at the aneurysm base may be obstructed by the WEB-device if not properly sized. Aneurysms treated with WEB-devices may show different kinds of recanalization compared to coiled aneurysms described by the WEB-occlusion scale[9].

Typical MRA sequences employed in this setting are non-contrast Time-of-Flight angiography (TOF), contrast enhanced angiography (CEA) and time-resolved CEA [8, 10]. Some institutions also use contrast-enhanced TOF, which offers higher signal-to-noise ratio, especially in small vessels [11]. However, visualization of the device and adjacent vessels with conventional MRI is limited due to the susceptibility artefacts, especially of the proximal and distal markers. Ultra-short echo time (UTE)-MRI may overcome this limitation due to the significantly reduced susceptibility to metal artifacts. Several studies have demonstrated the usefulness of an ultra-short echo time (UTE) sequence for follow-up of intracranial aneurysms treated with stents, coils and flow diverters using arterial spin-labelling based TOF with zero TE [12-15].

In this study, we assess the usefulness of a fast radial 3D-UTE research application sequence for follow-up of intracranial aneurysms treated with a WEB device with regard to visualization of the device, potential recanalization and adjacent structures.

MATERIALS AND METHODS

This prospective pilot study was designed to evaluate the usefulness of a 3D radial center-out UTE research application sequence in patients having undergone aneurysm treatment using the WEB device. The application of this sequence for research purposes was approved by the local Ethics Review board.

We prospectively included 12 consecutive patients, who had undergone therapy of an intracranial aneurysm using the WEB device between November 2020 and May 2022. These patients were either imaged within 24h after WEB implantation or during scheduled routine clinical and MRI follow-up 12 months after WEB implantation. All patients were given an explanation of the nature of the investigation prior to the MRI and written informed consent was obtained. All methods were applied in accordance with relevant guidelines and regulations (Declaration of Helsinki). In the study database all personal information was deleted to protect privacy.

For these patients, we collected standard demographic data including sex and age as well as data on any intracranial procedures performed, including the date, vessel site and device used for the WEB intervention.

Imaging

The 3D isotropic UTE sequence under investigation uses the following scan parameters: repetition time and echo time: 4.6 ms/0.04 ms; flip angle: 5 degrees; field of view: 230 x 230 mm²; matrix: 384 x 384; slice thickness: 0.6 mm; acquisition time: 2 minutes 58 seconds. The images were acquired in the axial plane.

We performed our standard protocol used for routine follow-up for aneurysm patients at our institution: 3D Fluid Attenuated Inversion Recovery (FLAIR), T2 Turbo Spin Echo (TSE), Diffused Weighted Imaging (DWI), Time-of-Flight (TOF) angiography, TOF angiography after i.v. administration of 7 ml of Gadobutrol (Gadovist, Bayer AG, Leverkusen) = TOF-CE. Additionally, the UTE sequence was performed after contrast administration. The scan parameters for our standard TOF sequence are the following: repetition time and echo time: 3.43 ms/20 ms; flip angle: 25 degrees; field of view: 210 x 210 mm²; matrix, 224 x 320; slice thickness: 0.6 mm; and acquisition time: 5 minutes 11 seconds.

All MRI exams were performed on the same 3T MAGNETOM Skyra Scanner (Siemens Healthcare, Erlangen, Germany) in all patients using a 32 channel head coil. The MRIs were performed between November 2020 and May 2022.

Invasive imaging: Standard biplanar digital subtraction angiography (DSA) was performed during WEB-implantation and during routine follow-up. In addition, flat-panel detector CT with intraarterial contrast administration was performed as well during WEB implantation and follow-up. DSA images were acquired within 24h to the MRI on one of our two angiography suites: Siemens Healthineers Axiom Artis or Philips Azurion (Philips, Amsterdam, Netherlands).

Image analysis

Two interventional radiologists (T.S. and D.T., with 16 and 10 years of experience, respectively, in radiology, as well as 9 and 5 years, respectively, in interventional neuroradiology) independently reviewed all imaging as an anonymized dataset in the standard picture archiving and communication system viewer (IMPAX EE, version R20 VIII SU1, Dedalus, Florence, Italy). The readers used multiplanar reformats (MPRs) in standard axial, sagittal and coronal as well custom planes for the MRI images and modified window widths and levels as needed on all images, including DSA. To avoid recall bias, an interval of at least 30 days was adhered to between reading the different datasets (TOF/ TOF-CE, UTE and DSA).

Artifact-related virtual stenosis

Artifact-related virtual stenosis of the parent vessel was assessed by performing an automated vessel analysis along the parent vessel including the base of the aneurysm (Fig. 1). The *syngo*.via vessel analysis tool was utilized (*syngo*.via, Siemens Healthcare, Erlangen, Germany). We extracted the minimum and maximum vessel diameter from the vessel analysis and compared it between MRI-modalities.

Virtual stenosis was calculated as follows:

$$(1 - \frac{MinVD}{MaxVD}) \times 100$$

Where MinVD refers to the minimum vessel diameter and MaxVD refers to the maximum vessel diameter.

Aneurysm occlusion

Occlusion of the treated aneurysms was evaluated according to the WEB occlusion scale (0, 0', 1, 2, 3, 1+3) . [16] This was assessed separately on the TOF/TOF-CE, the UTE and DSA images. After individual rating, we performed consensus reading for all cases.

Visualization of the WEB-device and adjacent vessels

The visibility of the WEB device configuration as well as the visualization of parent vessels were rated on a three-point Likert scale of 1 to 3 (3: excellent, 2: good, 1: poor). The criteria were the ability to visualize 1) both markers of the WEB device in order to facilitate understanding of device orientation, 2) the configuration of the WEB device in order to detect changes in configuration over time, and 3) the depiction of the borders of the WEB device towards the lumen of the adjacent vessels to detect protrusion and aneurysm recanalization. If all criteria were met, a score of 3 was applied, if one criterion was not satisfyingly visualized, a score of 2, and if two or more criteria were poorly or not visible, a score of 1 was given. This rating was performed on the TOF images and the UTE images separately and in consensus (Table 2). The WEB configuration, orientation and the relationship of the device to the parent vessel were compared to the gold-standard DSA (2D and 3D DSA).

Statistical analysis

Interreader reliability was assessed using Cohen`s kappa statistics (0.1-0.2: slight agreement, 0.21-0.4 fair agreement, 0.41-0.6: moderate agreement, 0.61-0.8: substantial agreement, 0.81-0.99: near perfect agreement).

Visibility of the WEB device and adjacent vessels measurements of UTE and TOF were compared using a Wilcoxon signed rank test.

Minimal vessel diameter results from the vessel analysis along the base of the aneurysm were assessed by two-sided student t-tests.

Consensus reading results of WEB recanalization visualized in UTE, TOF, TOF post contrast were compared to DSA results using a Wilcoxon signed rank test.

Statistical significance levels were set at $p<0.1$ due to the low number of patients.

RESULTS

We included 12 consecutive patients with 15 treated aneurysms. These 12 patients underwent 18 MRI examinations. TOF MRA was available in all MRI examination, TOF-CE was available in 17 out of 18 examinations and UTE in all MRI examinations. DSA was available in all imaging visits.

The demographics are summarized in Table 1. The median (range) age was 65 years (53-78). Six aneurysms were located in the anterior communicating artery (ACoA), six in the basilar artery (BA), two in the middle cerebral artery (MCA; one on the right, one on the left side) and one at the origin of the posterior communicating artery (PCom).

Table 1: Summary of demographics and aneurysm location (ACoA: anterior communicating artery, BA: basilar artery, MCA: middle cerebral artery, PCom: posterior communication artery) of 12 patients with 15 aneurysms.

Age	65 (8.5)
Female sex	9 (75%)
Aneurysm location	
ACoA	6
BA	6
C	2
Z	1

The WEB devices used ranged from 4.5 x 3 mm to 10 x 5 mm with an average diameter of 7.8 mm and an average height of 4.2 mm. Coils were used in addition to the WEB device in two cases and a self-expandable stent (Neuroform Atlas, Stryker Neurovascular, Kalamazoo, USA) was used in one case.

13 MRI exams were performed within 24h after WEB-implantation. 5 MRI exams were performed during follow-up. Of these, three were performed after 12 months during a one-day visit before the same-day MRI and two were performed during treatment of additional aneurysms. The average follow-up interval was 8 months.

Artifact-related virtual stenosis

The minimal diameter of the parent vessel was located at the level of the proximal WEB-marker in all cases (Figs. 1-4). The susceptibility of the proximal marker resulted in an average virtual stenosis of 38% in TOF-MRA, of 33% in CE-TOF and of 13% in UTE-MRI.

Aneurysm occlusion

Residual filling of the aneurysm adjacent to the WEB device was visible in 8 of 18 cases in DSA, which was used as the gold standard. The grade of occlusion was 0 in 9 exams, 0' in two exams, 1 in three exams, 2 in one exam, 3 in two exams and 1+3 in one exam.

With TOF MRA, 16 out of 18 cases were graded correctly. In two cases, occlusion was overestimated in TOF (1 instead of 3 and 1+3 respectively). With TOF-CE, 16 out of 17 cases were graded correctly (one occlusion overestimation grade 1 instead of 3) and with UTE, 17 out of 18 cases were graded correctly (one occlusion overestimation 0 instead of 0`).

Visualization of the WEB-device and adjacent vessels

The visualization of the WEB device position and configuration was rated as good (3) on the UTE sequence in 14 of 18 cases and as intermediate (2) in the remaining 4. Visualization on the TOF sequence was rated as intermediate (2) in 6 patients and poor (1) in the remaining 12 (Figs. 1,2,4). These data are summarized in Table 2.

Table 2: WEB visibility and parent vessel visibility were rated on a three-point Likert scale of 3 to 1 (3: excellent, 2: good, 1: poor).

MRI Scan	WEB Visibility Rating (UTE)	WEB Visibility Rating (TOF)	Parent Vessel Visibility (UTE)	Parent Vessel Visibility (TOF)
1	3	2	2	3
2	3	2	3	2
3	3	1	2	2
4	3	1	3	2
5	3	2	3	2
6	3	1	3	3
7	3	1	3	2
8	3	1	3	2
9	3	1	3	2
10	2	2	3	2
11	3	1	3	2
12	2	1	3	3
13	3	1	2	2
14	2	1	3	0
15	2	1	3	2
16	3	2	3	3
17	3	2	2	2
18	3	1	3	1

Statistical analysis

Interreader reliability regarding all imaging modalities was 0.67 (substantial agreement).

Visibility of the WEB device and adjacent vessels was significantly greater with UTE (median: 3) compared to TOF (median: 2; p=0.008).

The virtual stenosis was significantly higher in TOF compared to UTE (p=0.0004) and also in CE-TOF compared to UTE-MRI (p=0.003).

No significant difference in WEB recanalization grading was detected between UTE and DSA (p=0.9) and between TOF post contrast and DSA (p=0.45). A statistically significant difference was present between TOF and DSA (p=0.059).

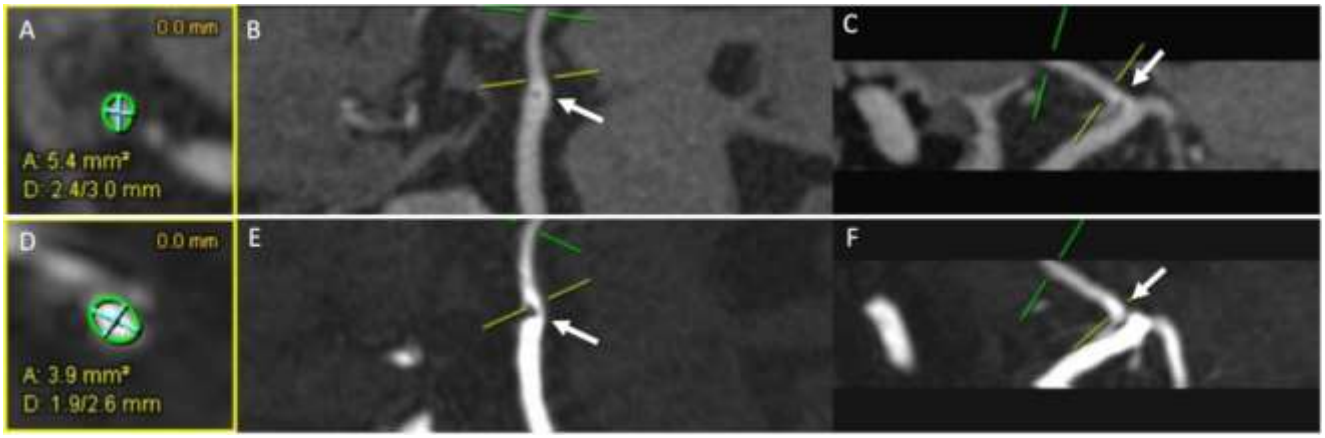

FIG 1. Representative case of the virtual stenosis analysis: The minimal diameter is calculated as transverse vessel surface in mm2 (A, B, C: UTE MRI, D, E, F: TOF MRA). Note the smaller cross-sectional surface vessel in TOF MRA (D-F) caused by the greater artefact of the WEB-detachment zone (arrows) compared to UTE MRI (A-C).

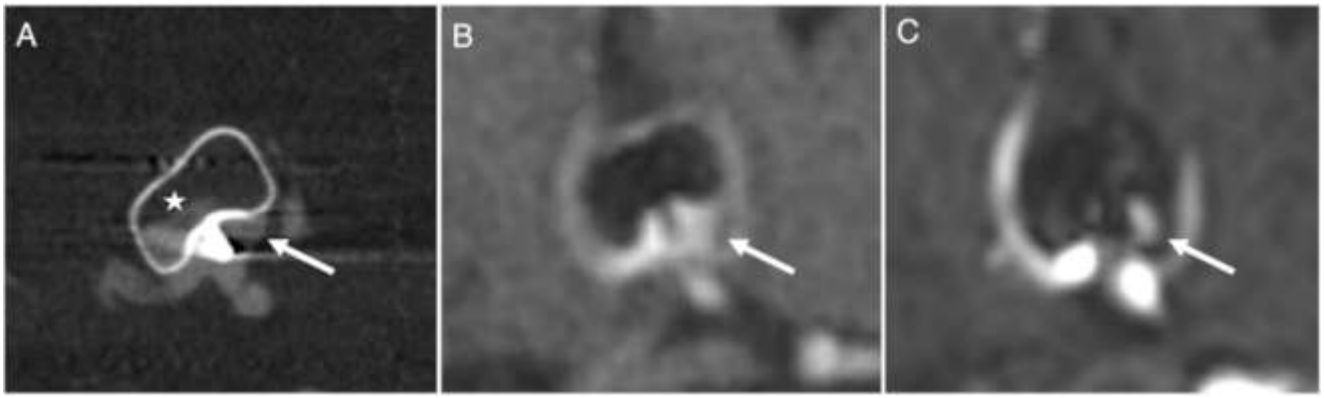

FIG 2. Follow-up of an incidental ACoA-Aneurysm treated with a WEB-device. Note the deformation of the WEB excellently depicted in FDCT (A, arrow) and UTE MRI (B, arrow). The shape of the WEB cannot be clearly visualized using TOF MRA after contrast administration (C). The perfusion within the WEB-device however cannot be visualized with neither MRI technique (asterisk in A) due to radio-frequency shielding effects.

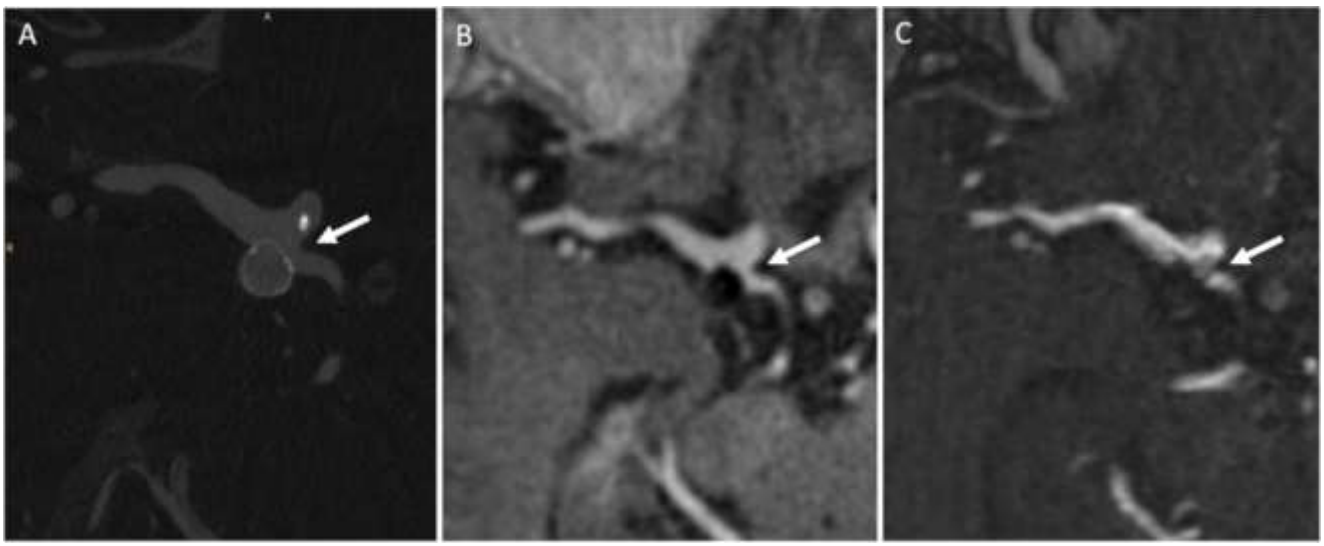

FIG 3. Posterior communicating artery-Aneurysm treated with WEB. The origin of the posterior communicating artery is well visualized in FD CT with intra-arterial contrast injection (A, arrow) and UTE MRI (B, arrow). In TOF MRA with contrast (C), the WEB detachment zone creates an artifact that does not allow clear visualization of the PCom-origin (arrows).

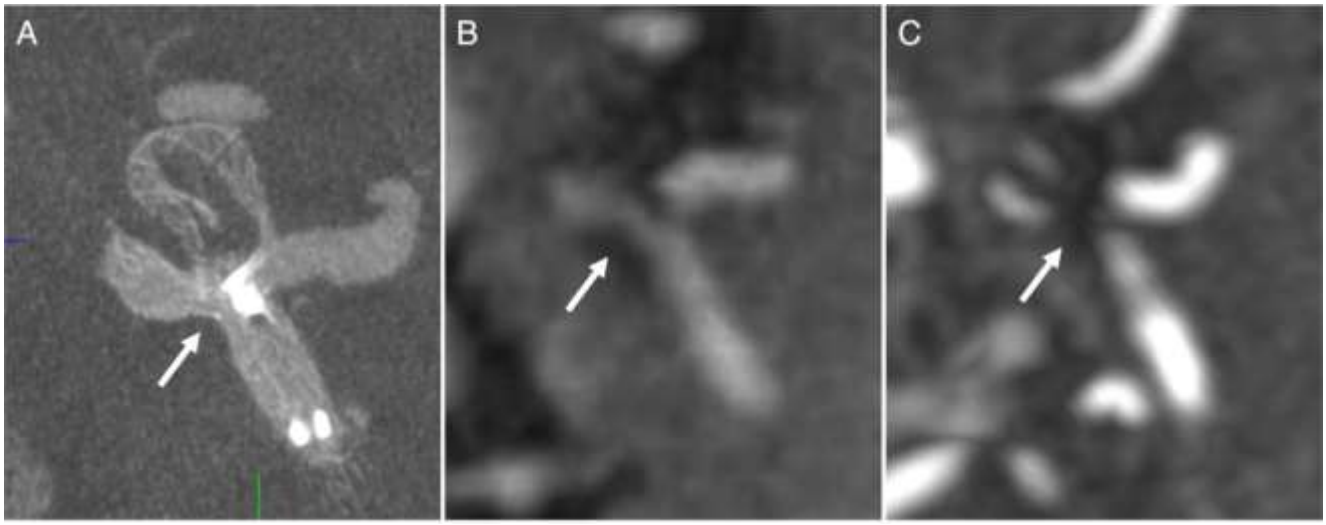

FIG 4. Example of an ACoA-Aneurysm treated with WEB and stent in the A1-A2 junction due to protrusion of the WEB after detachment. Note the visualization of the patent stent lumen in FD CT with intra-arterial contrast injection (A) and UTE MRI (B, arrow). In contrast-enhanced TOF MRA (C), the in-stent lumen adjacent to the proximal marker cannot be visualized (arrows).

DISCUSSION

In this study, we showed that UTE-MRI is able to superiorly visualize intra-aneurysmal WEB-devices and adjacent vessels compared to routine follow-up MRI with TOF without or with injection of Gadolinium containing contrast media with DSA as gold-standard. This is as well reflected by the significantly lesser degree of artifact-induced virtual vessel stenosis at the level of the proximal WEB-marker in UTE compared to TOF-MRA.

UTE MRI and TOF CE performed comparably well in grading of aneurysm recanalization, with TOF MRA without contrast being slightly inferior, however this did not reach statistical significance.

The main findings or our study are most likely due to the strong susceptibility of the proximal and distal markers of the WEB-device. The magnetic field distortion around the markers leads to variations in precessional frequency and subsequently signal loss due to T2* dephasing. This leads to severe artifacts in conventional MR-imaging, especially gradient-echo sequences such as TOF-MRA. Furthermore, susceptibility artifacts increase with field strength, which is especially relevant for the examination of intracranial aneurysms, where 3T has shown to be superior to 1.5T [17 18].

This explains the limitations of TOF-MRA in visualization of the WEB-device and the adjacent vessels at the aneurysm neck. The higher sensitivity to magnetic field variations is illustrated through the effect of a virtual stenosis in TOF-MRA.

UTE-MRI has a low sensitivity to susceptibility artefacts due to the very short echo time, which has been exploited for imaging of the bones and lung parenchyma [19, 20]. Several studies have also shown the usefulness of short echo-time sequences with spin labelling (SILENT-MRA) or intravenous contrast injection (UTE-MRA) after endovascular introduction of various metallic implants apart from WEB devices. Irie et al demonstrated the use of SILENT-MRA in nine patients treated with stent-assisted coiling with significantly higher subjective visibility compared to TOF imaging [12]. Takano et al reported on the use of SILENT-MRA in seven patients treated with Y-configuration stent-assisted coiling and 31 patients treated with Low-Profile Visualized Intraluminal Support (LVIS) stent-assisted coiling, in each case showing substantially better depictability of neck remnant perfusion than on TOF imaging [14, 15]. Oishi et al showed the superiority of SILENT-MRA in visualizing blood flow inside the flow diverting stent compared to TOF in 78 patients [13]. One study has used non contrast-enhanced sub-UTE-MRA in six patients after therapy with a flow diverting stent and was able to confirm better visualization as well [21]. In addition, time-resolved CEA seem to be beneficial for the follow-up especially in stent-assisted coil-embolization [22, 23].

Our report showed that combining contrast administration with a UTE sequence is useful for follow-up of intracranial aneurysms treated with the WEB device. Due to the use of intravenous contrast instead of spin labelling and subtraction, the structure of the WEB device can be entirely visualized, which would not be possible with SILENT-MRA. The most clinically relevant differences compared to TOF were the better ability to depict changes in device configuration that may lead to recanalization, and the better ability to judge the patency of parent arteries. Recanalization within the WEB device was not visible with neither TOF nor UTE MRI and might be due to the inherent magnetic RF-shielding effect.

Depicting the shape and the relation of the WEB-device to the parent vessels in non-invasive imaging is relevant, as protrusion of the device requires antithrombotic treatment [4]. The WEB-device is designed for broad-based aneurysms and with increasing operator experience, more complex aneurysms are treated. In highly complex aneurysms with branch-incorporation, a certain degree of protrusion is inevitable. This is reflected by the preparation of elective WEB-cases with dual antiplatelet therapy by some operators [4].

UTE MRI might show benefit as well for the assessment of coiled aneurysms. Even though the susceptibility of coils is highly inferior

compared to the WEB-device, small vessel branches in vicinity to the coilpack or the parent vessel after stent-assisted coiling can be challenging to evaluate on TOF-MRA.

There are limitations to this study. The number of patients included in this feasibility study is relatively low, which increases the risk of evaluation bias for comparison. The better visibility of the WEB-device and the lesser degree of virtual stenosis did not result in changes in patient-management in this small feasibility study. Furthermore, no significant difference between UTE and TOF was detected regarding aneurysm occlusion. However, the present study shows that an appropriately powered comparative study regarding aneurysm occlusion would require a larger number of patients.

CONCLUSIONS

UTE-MRI enables improved visualization of intraaneurysmal WEB-devices than routine follow-up MRI with TOF. The most clinically relevant differences were the ability to judge the patency of vessels at the aneurysm neck and to depict changes in device configuration that may lead to recanalization. Adding UTE MRI to MRI protocols after treatment of intracranial aneurysms treated with the WEB device may be beneficial to depict changes in configuration as well as recanalization and does not excessively extend scan time due to the short acquisition.

ACKNOWLEDGMENTS

REFERENCES

1. Hendricks BK, Yoon JS, Yaeger K, et al. Wide-neck aneurysms: systematic review of the neurosurgical literature with a focus on definition and clinical implications. *J Neurosurg* 2019;133:159-165
2. De Leacy RA, Fargen KM, Mascitelli JR, et al. Wide-neck bifurcation aneurysms of the middle cerebral artery and basilar apex treated by endovascular techniques: a multicentre, core lab adjudicated study evaluating safety and durability of occlusion (BRANCH). *J Neurointerv Surg* 2019;11:31-36
3. Brinjikji W, Murad MH, Lanzino G, et al. Endovascular treatment of intracranial aneurysms with flow diverters: a meta-analysis. *Stroke* 2013;44:442-447
4. Goyal N, Hoit D, DiNitto J, et al. How to WEB: a practical review of methodology for the use of the Woven EndoBridge. *J Neurointerv Surg* 2020;12:512-520
5. Larsen N, Fluh C, Madjidyar J, et al. Visualization of Aneurysm Healing : Enhancement Patterns and Reperfusion in Intracranial Aneurysms after Embolization on 3T Vessel Wall MRI. *Clin Neuroradiol* 2020;30:811-815
6. van Rooij S, Peluso JP, Sluzewski M, et al. Mid-term 3T MRA follow-up of intracranial aneurysms treated with the Woven EndoBridge. *Interv Neuroradiol* 2018;24:601-607
7. van Amerongen MJ, Boogaarts HD, de Vries J, et al. MRA versus DSA for follow-up of coiled intracranial aneurysms: a meta-analysis. *AJNR Am J Neuroradiol* 2014;35:1655-1661
8. Algin O, Yuce G, Koc U, et al. A comparison between the CS-TOF and the CTA/DSA for WEB device management. *Interv Neuroradiol* 2022;28:29-42
9. Lubicz B, Klisch J, Gauvrit JY, et al. WEB-DL endovascular treatment of wide-neck bifurcation aneurysms: short- and midterm results in a European study. *AJNR Am J Neuroradiol* 2014;35:432-438
10. Akkaya S, Akca O, Arat A, et al. Usefulness of contrast-enhanced and TOF MR angiography for follow-up after low-profile stent-assisted coil embolization of intracranial aneurysms. *Interv Neuroradiol* 2018;24:655-661
11. Ozsarlak O, Van Goethem JW, Parizel PM. 3D time-of-flight MR angiography of the intracranial vessels: optimization of the technique with water excitation, parallel acquisition, eight-channel phased-array head coil and low-dose contrast administration. *Eur Radiol* 2004;14:2067-2071
12. Irie R, Suzuki M, Yamamoto M, et al. Assessing Blood Flow in an Intracranial Stent: A Feasibility Study of MR Angiography Using a Silent Scan after Stent-Assisted Coil Embolization for Anterior Circulation Aneurysms. *AJNR Am J Neuroradiol* 2015;36:967-970
13. Oishi H, Fujii T, Suzuki M, et al. Usefulness of Silent MR Angiography for Intracranial Aneurysms Treated with a Flow-Diverter Device. *AJNR Am J Neuroradiol* 2019;40:808-814
14. Takano N, Suzuki M, Irie R, et al. Usefulness of Non-Contrast-Enhanced MR Angiography Using a Silent Scan for Follow-Up after Y-Configuration Stent-Assisted Coil Embolization for Basilar Tip Aneurysms. *AJNR Am J Neuroradiol* 2017;38:577-581
15. Takano N, Suzuki M, Irie R, et al. Non-Contrast-Enhanced Silent Scan MR Angiography of Intracranial Anterior Circulation Aneurysms Treated with a Low-Profile Visualized Intraluminal Support Device. *AJNR Am J Neuroradiol* 2017;38:1610-1616
16. Caroff J, Mihalea C, Tuilier T, et al. Occlusion assessment of intracranial aneurysms treated with the WEB device. *Neuroradiology* 2016;58:887-891
17. Gibbs GF, Huston J, 3rd, Bernstein MA, et al. Improved image quality of intracranial aneurysms: 3.0-T versus 1.5-T time-of-flight MR angiography. *AJNR Am J Neuroradiol* 2004;25:84-87
18. Kwak Y, Son W, Kim YS, et al. Discrepancy between MRA and DSA in identifying the shape of small intracranial aneurysms. *J Neurosurg* 2020;134:1887-1893
19. Robson MD, Gatehouse PD, Bydder M, et al. Magnetic resonance: an introduction to ultrashort TE (UTE) imaging. *J Comput Assist Tomogr* 2003;27:825-846
20. Bergin CJ, Pauly JM, Macovski A. Lung parenchyma: projection reconstruction MR imaging. *Radiology* 1991;179:777-781
21. Ayabe Y, Hamamoto K, Yoshino Y, et al. Ultra-short Echo-time MR Angiography Combined with a Subtraction Method to Assess Intracranial Aneurysms Treated with a Flow-diverter Device. *Magn Reson Med Sci* 2021
22. Boddu SR, Tong FC, Dehkharghani S, et al. Contrast-enhanced time-resolved MRA for follow-up of intracranial aneurysms treated with the pipeline embolization device. *AJNR Am J Neuroradiol* 2014;35:2112-2118
23. Choi JW, Roh HG, Moon WJ, et al. Time-resolved 3D contrast-enhanced MRA on 3.0T: a non-invasive follow-up technique after stent-assisted coil embolization of the intracranial aneurysm. *Korean J Radiol* 2011;12:662-670

SUPPLEMENTAL FILES